A 1.9GHz RF Transmit Beacon using Environmentally Scavenged Energy

Shad Roundy†, Brian P. Otis*, Yuen-Hui Chee*, Jan M. Rabaey*, Paul Wright†
*Department of Electrical Engineering and Computer Sciences
†Mechanical Engineering Department
University of California, Berkeley
2108 Allston Way, Suite 200, Berkeley, CA 94704
shadr@kingkong.me.berkeley.edu

ABSTRACT

The design and implementation of a 1.9GHz radio frequency transmit beacon is presented. The beacon is completely self-contained, and all necessary energy is scavenged through solar and vibrational energy sources. Custom RF integrated circuitry and energy scavenging devices are used to create a highly integrated and efficient beacon. The 1.9GHz direct modulated transmitter uses a micromachined resonator and requires no other external components, inductors, or crystals. The beacon achieves duty cycles up to 100% for typical ambient solar conditions and 2.6% for typical ambient vibrational conditions.

1. INTRODUCTION

Over the past few years there has been an increasing focus in the research community on ad-hoc, low power, wireless sensor networks [1]. In fact, it is widely believed that the next revolution in computing technology will be the widespread deployment of small wireless computing and communication devices that will integrate seamlessly into daily life [2]. Wireless sensor networks have recently gained exposure as a means to increase the efficiency, comfort, and/or security of buildings and other infrastructures [3]. The ultimate goal is to improve the comfort and health of indoor environments while simultaneously decreasing the energy use of these buildings. By improving indoor environments, it has been estimated that the US could realize annual health and productivity savings of up to $200 billion [4].

The proliferation of such sensor networks relies on low power wireless nodes, which must be completely autonomous and maintenance free. Thus, the energy necessary for node operation must be scavenged directly from the environment. For such a system, node-to-node RF communication is required. Scavenging enough energy from the environment to enable an RF link is one of the main challenges in implementing a complete wireless sensor network. This paper describes the design and implementation of a self-contained 1.9GHz RF transmit beacon, demonstrating the feasibility of sensor network deployment using vibration and solar energy scavenging techniques.

2. ENERGY SCAVENGING MECHANICAL STRUCTURES

2.1 Potential Energy Scavenging Sources

Since the entire energy consumption of the RF electronics must be scavenged from the environment, the choice of energy scavenging technology is crucial. A number of approaches to energy scavenging have been studied over the past few years. Naturally occurring temperature variations are one potential source of power. For example, Stordeur and Stark [5] have demonstrated a thermoelectric device that can produce 15 μW of power from a 10° C temperature differential. Other researchers have focused on scavenging power from the human body. Shenck and Paradiso [6] have built shoe inserts capable of generating 8.4 mW of power under normal walking conditions. Mechanical vibrations are another promising power source. Amirtharajah and Chandrakasan [7] have demonstrated an electromagnetic vibration-to-electricity converter with a $(4x4x10)cm^3$ volume that produces 400 μW of power (or 2.5 $\mu W/cm^3$). Both Meninger *et al* [8] and Roundy *et al* [9] have published electrostatic MEMS designs with simulated power outputs in the range of tens of microwatts per cubic centimeter. Finally, Ottman *et al* [10] have designed and optimized power circuitry to be used with a piezoelectric vibration based generator. An enormous amount of research has been focused on solar power. A good summary of solar (photovoltaic) technology specifically applied to indoor environments is the recent work by Randall [11]. A more complete comparison of potential power scavenging sources is published elsewhere [12].

Figure 1 shows a comparison of the potential output versus lifetime from solar cells, generators based on mechanical vibrations, and various battery chemistries.

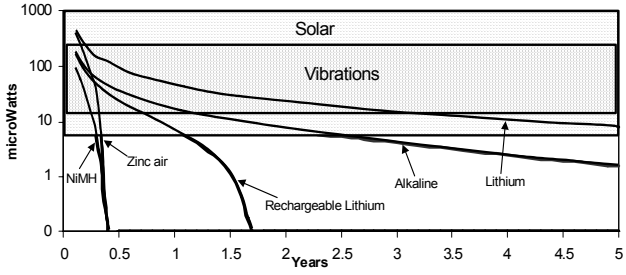

Figure 1. Power Density ($\mu W/cm^3$) vs. lifetime for batteries, solar cell, and vibration based power.

The two boxes shown in the figure represent the range of power available from solar cells and vibrations. The top of the solar regime represents the power typically available in mid-day sun. The bottom of the solar box represents available power in normal office lighting environments. The vibration regime represents the range of power available from a variety of low-level vibration sources ranging from the ductwork in buildings to small household appliances such as a microwave oven. The average power available does not depend on the projected lifetime of the device for either solar or vibration based power

sources. Figure 1 clearly shows that if the projected lifetime of a device is greater than about 1 year, solar cells and vibrations offer a better power source than a primary battery.

The goal of this work was to develop a completely self-powered wireless node. The two energy scavenging technologies that seem most applicable are solar power and vibration-based power due to the large potential application space of these technologies. Photovoltaics are a mature technology, and a solar cell based power source can be implemented using commercial off-the-shelf technology. However, less work has been done on exploiting low-level vibrations as a power source for low power electronics. While both solar and vibration based power sources are presented here, the development of the vibration-to-electricity converter used in the vibration based power train represents a significant research contribution in itself.

2.2 Vibration-to-Electricity Conversion

A wide variety of vibration sources have been considered and measured in an effort to estimate realistic potential for power generation. Measured sources include HVAC ducts, large industrial equipment, small household appliances, large exterior windows, office building floors, and automobiles. A fairly representative vibration input of 2.25 m/s^2 (0.23g) at 60 Hz was used for this analysis.

Three potential methods of coupling the mechanical kinetic energy to electrical energy exist: electromagnetic (inductive), electrostatic (capacitive), and piezoelectric. Given the constraints of the project (size, voltage, etc.), piezoelectric converters are the most attractive [12].

A two layer piezoelectric bender mounted as a cantilever beam was selected as the preferred design topology because of the high strains and low resonant frequencies that such a topology produces. The piezoelectric generator, terminated with a simple resistive load, can be modeled as a relatively simple third order dynamic system. The system equations are given below.

$$\ddot{\delta} = \frac{-k_{sp}}{m}\delta - \frac{b_m b^{**}}{m}\dot{\delta} + \frac{k_{sp} dn}{m t_c} V + b^* \ddot{y} \quad (1)$$

$$\dot{V} = \frac{-Y d t_c}{n\varepsilon}\dot{\delta} - \frac{1}{RC_p} V \quad (2)$$

where δ is the average strain in the material, k_{sp} is the effective spring constant, b_m is the damping coefficient, b* and b** are a geometric constants, m is the proof mass, t_c is the thickness of the piezoelectric layers, d is the piezoelectric strain coefficient, n is the number of piezoelectric layers, V is the voltage across the load resistor, Y is the elastic modulus, ε is the dielectric constant, R is the load resistance, C_p is the capacitance of the piezoelectric generator and $\ddot{y}$ represents the input vibration. The simulated and measured power output versus the load resistance for an initial prototype device is shown in Figure 2. The effective damping induced on the vibrating piezoelectric structure by the electrical load is a function of the resistance R. Optimal power transfer to the load occurs when the electrically induced damping is equal to the mechanical damping inherent in the system. A closed form solution for the optimal load resistance can be derived from equations 1 and 2, and is shown as equation 3. The measured data fits the simulated data sufficiently well to use the model as a basis for design optimization.

$$R_{opt} = \frac{1}{\omega C_p}\frac{2\zeta}{\sqrt{4\zeta^2 + k^4}} \quad (3)$$

where ω is the frequency of the driving vibrations, ζ is the dimensionless damping ratio, and k is the piezoelectric coupling coefficient.

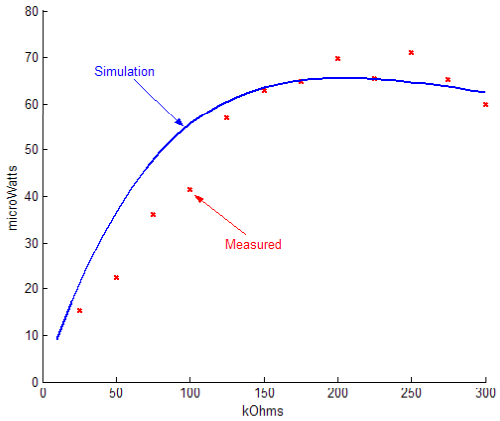

Figure 2. Measured and simulated power output vs. load resistance

The design dimensions were then formally optimized using the power estimated from a dynamic simulation of equations 1 and 2 as the objective function. The design was constrained to a total size of 1 cm^3 and a total length of 3 cm. The resulting converter is shown in Figure 3.

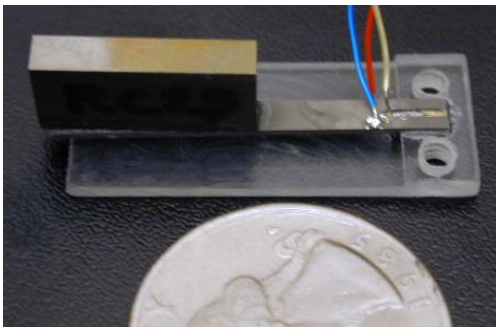

Figure 3. Optimized Piezoelectric Generator

The maximum power from this converter into a purely resistive load with driving vibrations of 2.25 m/s^2 at 60 Hz is 375 µW. A more representative situation is to connect the generator to a capacitive load through a full wave rectifier. The power transferred to a 3.3µF load capacitor is shown in Figure 4. The effectiveness of the power transfer to the capacitive load depends on the voltage across the storage capacitor (V_{st}). Therefore, the power data in Figure 4 is shown as a function of the ratio between V_{st} and the open circuit voltage of the piezoelectric converter (V_{oc}) under the same driving vibrations. The maximum power transfer generally occurs when this ratio is very close to 0.5. The maximum power delivered to the capacitive load is 180 µW, or about half that delivered to a purely resistive load.

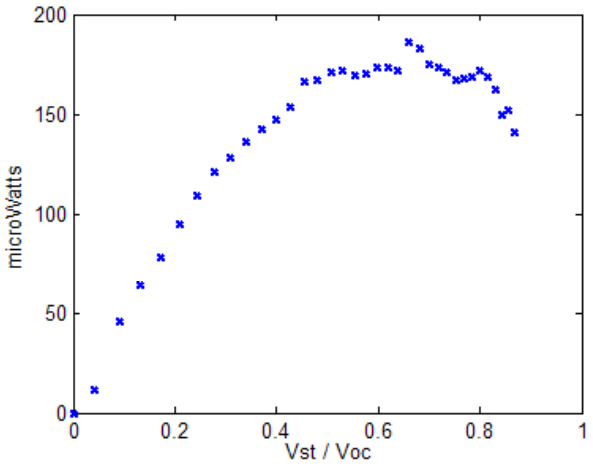

Figure 4. Measured power transferred to a 3.3 µF capacitive load vs. ratio of storage (V_{st}) to open circuit (V_{oc}) voltage.

2.3 Solar Scavenging

A thin-film cadmium telluride (CdTe) solar cell was chosen due its good performance under a wide range of light conditions. Single crystal solar cells offer efficiencies of about 15% for inexpensive commercially available cells and over 20% for high-end research cells [11]. However, single crystal cells do not perform well in indoor environments due to severe degradation of the open circuit voltage. Thin-film polycrystalline cells, which exhibit efficiencies of 10 – 13%, are also available. Thin-film amorphous silicon solar cells have a lower efficiency ranging from 8 – 10%, but are well suited for indoor applications because their spectral response closely matches that of fluorescent white light [11]. The efficiency of CdTe cells ranges from 8 – 13%. CdTe cells have a very wide spectral response, and so perform well both in both indoor and outdoor environments. For this reason, a thin-film CdTe cell was chosen for this project. The particular solar array chosen is a Panasonic BP-213318 thin-film CdTe on glass module comprised of 5 cells in series and measures approximately (3x2)cm^2. (See Figure 10 below.)

3. ENERGY SCAVENGING CIRCUITRY

3.1 Power Circuitry Functionality

The power circuitry converts the scavenged energy into a stable supply voltage for the RF circuitry. This entails converting a high impedance, unstable supply into a stable, low impedance 1.2V supply. The storage capacitor, C_{st}, in Figure 5 functions as an energy reservoir. When the capacitor charges to a pre-specified energy level, the supply rails to the RF circuitry are activated and energy is consumed. Because the transmitter dissipates power faster than the piezoelectric generator or solar cell produces it, the voltage across the storage capacitor falls when the radio is on. Once the energy has been depleted to a level specified by the "Shutdown control" block, the supply rails are disabled and the capacitor is recharged.

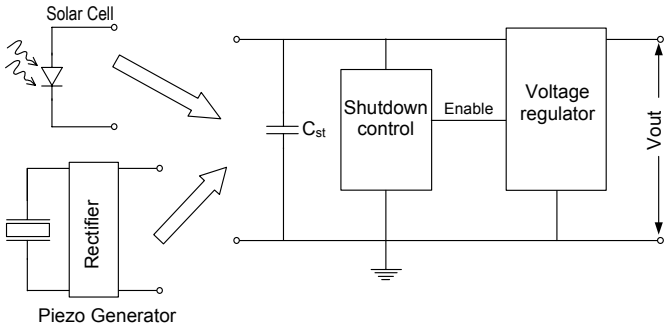

Figure 5. Power conditioning circuit

3.2 Energy Storage and Voltage Regulation

Though the circuit shown in Figure 5 uses a capacitor as an energy storage element, a rechargeable battery could also be used in a very similar circuit. Batteries have far higher energy density than capacitors. For example, rechargeable lithium ion batteries have an energy density of roughly 1000 J/cm^3. Ceramic capacitors have an energy density on the order of 1 to 10 J/cm^3. However, most lithium ion batteries are limited to 500 to 1000 recharge cycles and have a limited shelf life. Furthermore, in our proposed application where the batteries are being charged with a trickle of current rather than being deeply discharged, lifetime will suffer. Capacitors, on the other hand, have an almost infinite lifetime and are simpler to charge. Because this application does not need much energy storage, and because lifetime of the node is a primary concern, a capacitor was used.

Efficiency is usually the primary consideration in the choice of a voltage regulator or DC-DC converter for extremely low power applications. Typical efficiencies for DC-DC converters are around 90%. By contrast, the efficiency of linear regulators depends on the ratio of input to output voltage. Simplicity is the primary advantage of linear regulators, which require almost no external components. DC-DC converters usually require a large external inductor on the order of 10 µH. Although a linear regulator results in a lower total efficiency in the current design scenario, a linear regulator was chosen because of its higher level of integration and increased simplicity.

3.3 Efficiency

The efficiency of the power circuitry may be estimated by the following equation.

$$\eta = \frac{P_{diss\_ave}}{P_{diss\_ave} + P_{loss\_reg} + P_{loss\_shutdown} + P_{loss\_rect}} \quad (4)$$

where P_{diss_ave} is the average power dissipation of the radio, P_{loss_reg} is the average power loss from the regulator, $P_{loss\_shutdown}$ is the average power loss from the shutdown control circuit, and P_{loss_rect} is the power loss from rectification which only applies to the piezoelectric generator, not the solar cell.

The average power dissipation and the power loss from regulation both depend on the duty cycle, which in turn depends on how much power is being generated. Numbers for three representative situations are shown in Table 1.

Table 1. Power Conversion Efficiency Under Various Operating Conditions

	Vibrations (2.25 m/s^2)		Fluorescent light.		Bright indoor lamp.	
	µW	%	µW	%	µW	%
P_{diss_ave}	192	50.1	64	62.5	1320	64.8
P_{loss_reg}	108	28.2	36	35.2	715	35.1
$P_{loss\_shutdown}$	2.4	0.6	2.4	2.3	2.4	0.1
P_{loss_rect}	80.7	21.1	NA	NA	NA	NA
Total loss	191	49.9	38.4	37.5	717.4	35.2

The overall efficiency could be improved if a DC-DC converter were used at the cost of increased size and complexity. Additionally, the efficiency of the power circuit could be improved if the operating voltage across the storage capacitor were increased.

4. ULTRA LOW POWER RF CIRCUITRY

Unlike passive RFID tags, sensor nodes must communicate with each other, not with sensitive, high power basestations. Thus, an entire ultra low power radio link must be formed. To achieve a 10m range and relax receiver sensitivity constraints, the chosen transmit power was 0dBm. Novel RF circuit design techniques were employed to achieve extremely low power consumption and a very high level of integration. This section describes the techniques used to enable ultra low power RF circuitry.

4.1 Oscillator/Modulator

Typical RF transmitters require many power hungry blocks, including a low frequency reference, phase detector, voltage controlled oscillator (VCO), frequency dividers, and mixers. Our implementation employs RF micro electro-mechanical (MEMS) technology to reduce the number of blocks needed to generate and modulate the carrier.

Using an Agilent Film Bulk Acoustic Resonator (FBAR), a low power 1.9GHz oscillator was developed that requires no low frequency reference or phase locked loop (PLL) [13][14]. See the block diagram in Figure 6 below.

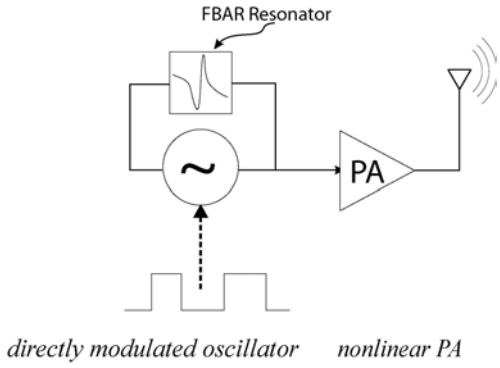

Figure 6. 1.9GHz Direct Modulation Transmitter Architecture

The CMOS oscillator is wirebonded to the resonator chip located approximately 200µm away using Chip-on-Board (COB) technology. This close chip placement reduces the parasitics associated with the wirebonding. See the transmitter photograph in Figure 7.

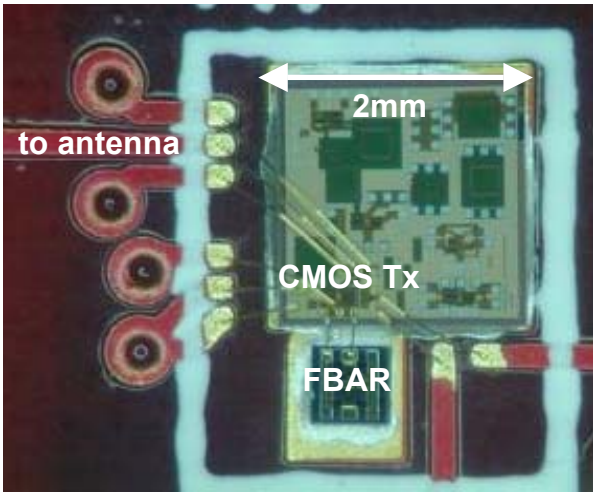

Figure 7. Photograph of Transmitter Chip-on-Board Assembly

Notice that no external components are required, including inductors or crystals. Instead of requiring a mixer to upconvert a baseband signal, the oscillator is directly modulated by the baseband on-off keyed signal. This results in significant savings in power consumption. The total power consumption of the oscillator/modulator is less than 400µW. This RF block supplies a 100mV (zero-peak) signal to the power amplifier, which is discussed in the next section.

4.2 Power Amplifier/Antenna

For a constant envelope modulated signal, a high efficiency non-linear amplifier can be employed. The fully integrated power amplifier boosts the RF signal from the oscillator and drives the antenna. It consists of a pre-amplifier, a driver and a class C output stage as shown in the schematic below.

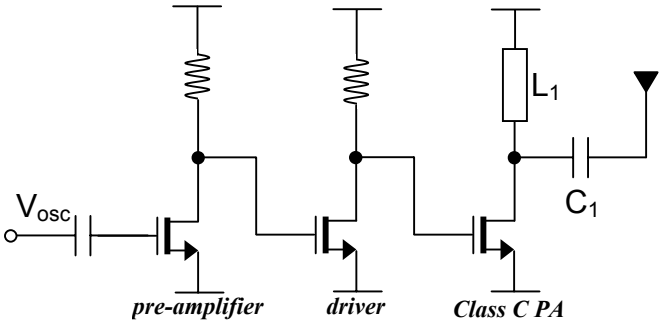

Figure 8. Non-Linear Power Amplifier

An on-chip inductor was employed, allowing a fully integrated RF transmitter. To reduce the die area, the capacitor C_1 is used to block the dc signal as well as to resonate with the inductor L_1 for frequency selection. The power amplifier delivers –1.5dBm to the antenna at 1.9GHz. The output spectrum of the transmitter is shown in Figure 9.

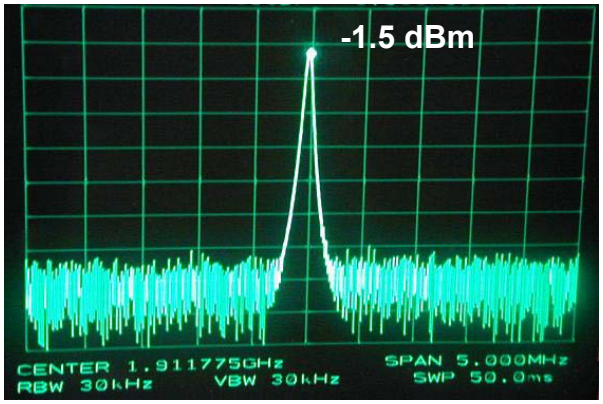

Figure 9. Transmitter Output Frequency Spectrum

A 1.9 GHz chip antenna from Rangestar was chosen for its small form factor and excellent radiation pattern.

5. EXPERIMENTAL RESULTS

The completed transmit beacon is shown in Figure 10 below. The beacon was tested with both solar and vibrational energy scavenging sources.

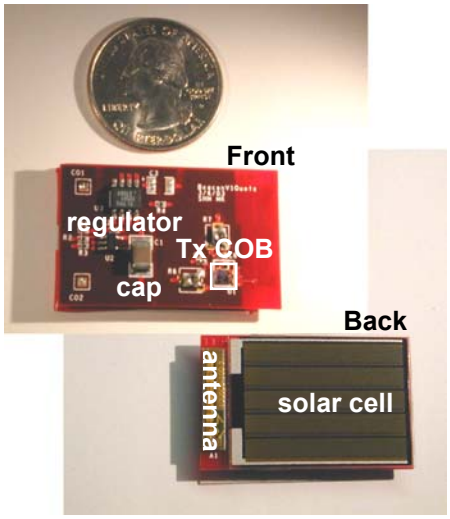

Figure 10. Integrated Transmit Beacon

As shown in the photographs above, the beacon contains a board mounted antenna, solar cell, regulator, energy storage capacitor, and a custom ultra low power 1.9GHz, –1.5dBm transmitter. The board dimensions are (2.4x3.9)cm^2. It operates on energy scavenged from light or vibrations; thus, no external supply or battery energy source is needed. The board requires no external voltages, references, or connections, and can operate indefinitely from energy scavenged from light or vibrations. Measured performance results will now be presented.

5.1 Transient Charge/Discharge Waveforms

As described in Section 3, the beacon charges the storage capacitor until the desired energy level is achieved. Then, on-board logic turns on the voltage regulator, enabling a 1.2V supply rail for the RF circuitry. The RF block transmits until the energy is depleted, and the process repeats. Measured waveforms are presented in Figure 11.

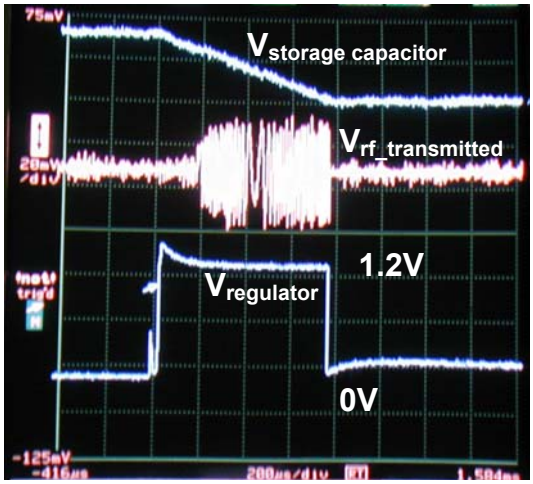

Figure 11. Beacon Waveforms under Low Light Conditions

These traces shown in Figure 11 result from beacon operation in low indoor lighting conditions, yielding a duty cycle of 0.36%. Under higher lighting conditions, the duty cycle increases accordingly. Figure 12 shows beacon operation under high indoor lighting conditions, achieving a duty cycle of approximately 11%.

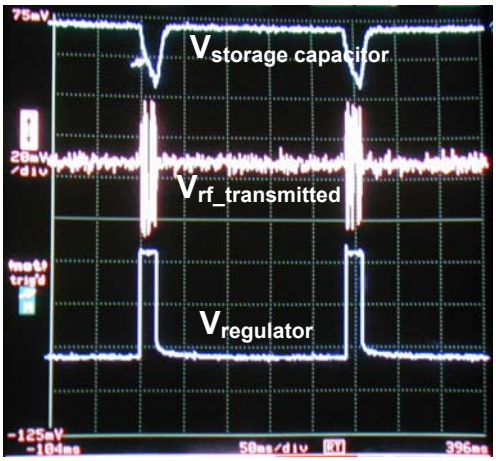

Figure 12. Beacon Waveforms under high light conditions

5.2 Measured Duty Cycle Performance

The performance of this system is best described by the duty cycle that the 1.9GHz transmitter can achieve. Table 2 presents the measured duty cycle of the transmit beacon in various lighting and vibration conditions.

Table 2. Measured Beacon duty cycles under various environmental conditions

Light Level	Duty Cycle
Low Indoor Light	0.36%
Fluorescent Indoor Light	0.53%
Partly Cloudy Outdoor Light	5.6%
Bright Indoor Lamp	11%
High Light Conditions	100%
Vibration Level	**Duty Cycle**
$2.2 m/s^2$	1.6%
$5.7 m/s^2$	2.6%

The piezoelectric generator is inherently a resonant structure. It is critical that the resonant frequency matches that of the input vibrations. Typically, the vibration environment is well characterized. Thus, the vibration generator is designed appropriately for a given vibration environment. Active tuning of the resonant frequency may be possible, and is a topic of further study. Figure 13 shows the beacon duty cycle achieved from the vibration generator versus frequency of the driving vibrations. The figure clearly shows the critical importance of matching the generator resonant frequency to the frequency of the input vibrations.

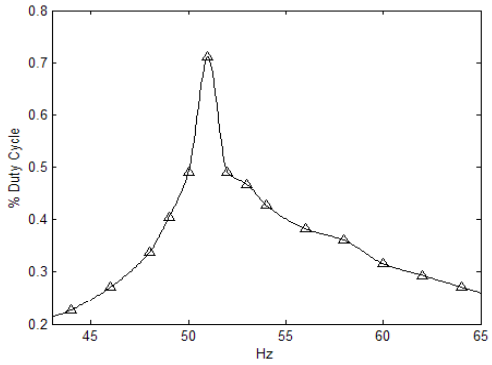

Figure 13. Beacon duty cycle vs. frequency of vibrational energy source.

6. CONCLUSIONS

A 1.9GHz transmit beacon has been designed and tested. The beacon is completely self-contained, and will run indefinitely on energy scavenged from ambient solar or vibration energy sources. To meet these goals, the following advancements have been made:

1. We have investigated solar and vibrational energy scavenging and have developed an optimized piezoelectric generator which delivers 180μW to a capacitive load at $2.25 m/s^2$.
2. A custom RF transmitter has been developed using micromachined resonators. The highly integrated 1.9GHz transmitter requires no external components and delivers –1.5dBm to an on-board chip antenna. A directly modulated oscillator is used which requires no up-conversion circuitry.
3. A very small form factor was achieved through highly integrated circuit design, careful board design, and a compact energy conversion system.

This work represents the confluence of technological advances made in energy scavenging and ultra low power RF circuit design. This demonstration proves the feasibility of completely self-contained, wireless sensor network communications.

7. ACKNOWLEDGMENTS

The authors would like to thank ST Microelectronics for the CMOS fabrication and Agilent Technologies for the FBAR fabrication. This research was funded in part by DARPA (grant nos. N66001-01-1-8967 and F33615-02-2-4005) and NSF (grant no. CMS-0088648).

8. REFERENCES

[1] Rabaey, J. M., Ammer, M. J., da Silva, J. L., Patel, D., Roundy S, "PicoRadio Supports Ad Hoc Ultra-Low Power Wireless Networking," *IEEE Computer*, Vol. 33, No. 7, p. 42-48.

[2] Gates, B., "The disappearing computer," *The Economist*, Special Issue, Dec. 2002, p. 99.

[3] J. Rabaey, J. Ammer, T. Karalar, S. Li, B. Otis, M. Sheets, T. Tuan, "PicoRadios for Wireless Sensor Networks: The Next Challenge in Ultra-Low Power Design," *IEEE ISSCC Digest of Technical Papers*, pp.200-1, Feb 2002.

[4] Fisk, W.J. 2000. "Health and productivity gains from better indoor environments and their implications for the U.S. Department of Energy." *Proceedings of the E-Vision 2000 Conference*, October 11-13, 2000, Washington, D.C.

[5] Stordeur, M., Stark, I., "Low Power Thermoelectric Generator – self-sufficient energy supply for micro systems," *16th Int. Conf. on Therm*, 1997, pp. 575-7.

[6] Shenck, N. S., Paradiso, J. A., 2001. "Energy Scavenging with Shoe-Mounted Piezoelectrics," *IEEE Micro*, 21 (2001) 30-41.

[7] Amirtharajah, R., Chandrakasan, A.P., "Self-Powered Signal Processing Using Vibration-Based Power Generation," *IEEE JSSC*, Vol. 33, No. 5, p. 687-695.

[8] Meninger, S., Mur-Miranda, J.O., Amirtharajah, R., Chandrakasan, A.P., and Lang, J.H. "Vibration-to-Electric Energy Conversion." *IEEE Trans. VLSI Syst*., 9(2001) 64-76.

[9] Roundy S., Wright P. K., Pister K. S. J., "Micro-Electrostatic Vibration-to-Electricity Converters", *ASME IMECE*, Nov. 17-22, 2002, New Orleans, Louisiana.

[10] Ottman G. K., Hofmann H. F., Lesieutre G. A., "Optimized piezoelectric energy harvesting circuit using step-down converter in discontinuous conduction mode," *IEEE Trans on Power Elect*, vol.18, no.2, 2003, pp.696-703.

[11] Randall, J. F., "On ambient energy sources for powering indoor electronic devices," Ph.D Thesis, Ecole Polytechnique Federale de Lausanne, May 2003.

[12] Roundy, S., Wright, P. K., and Rabaey, J., "A Study of Low Level Vibrations as a Power Source for Wireless Sensor Nodes", *Computer Communications*, vol. 26, no. 11, 2003, pp 1131 - 1144.

[13] R. Ruby, P. Bradley, J. Larson III, Y. Oshmyansky, D. Figueredo, "Ultra-miniature high-Q filters and duplexers using FBAR technology", *IEEE ISSCC Digest of Technical Papers*, pp.120-1, Feb. 2001.

[14] B. Otis and J. Rabaey, "A 300μW 1.9GHz oscillator utilizing micromachined resonators," *IEEE Proceedings of the 28th ESSCIRC*, vol. 28, Sept. 2002.